Supporting Information

Highly transparent poly(glycidyl methacrylate-*co*-acryloisobutyl POSS) for 100 μm-thick submicron patterns with an aspect ratio over 100

Kwanghyun Kim,[a] Sunyoung Yu,[a] Sung-Wook Kim,[a] Taegeon Kim,[b] Sang-Min Kim,[b] Se-Young Kang,[a] Seung Min Han*,[b] and Ji-Hyun Jang*,[a]

Materials

GMA was purchased from Alfa Aesar and used without further purification. Acryloisobutyl-POSS (A1-POSS) was obtained from Hybrid Plastics. AIBN was purchased from Samchun and purified by recrystallization from methanol. Distilled THF was used as a solvent for the synthesis reaction.

Characterizations

The synthesized polymers were characterized by scanning electron microscopy (FEI Nano 230 and Hitachi High-Technologies S-4800), Fourier-transform infrared spectroscopy (FT-IR, Varian 670/620), nuclear magnetic resonance spectroscopy (NMR, Agilent 400-MR DD2), gel permeation chromatography (GPC, Wyatt miniDAWN TREOS), and UV-Vis spectroscopy (Agilent Cary 5000). Mechanical properties of submicron structures were investigated via nanoindentation (Hysitron Ti-750) using a Berkovich tip and the Oliver–Pharr method[1] to analyze the data to determine the respective Young's modulus and hardness values.

Patterning with photoresist

Samples for the patterning of PGMAs and PGPs were prepared by the following procedure. 15 x 15 mm size of SiO_2/Si wafer was used as a substrate after washing step by step in acetone, IPA, D.I. water, and ethanol followed by N_2 blowing. A 30 wt% solution of the PGPs in cyclopentanone was spin-coated at a speed of 750 rpm for 1 min. The samples were prebaked at 75 ^oC for 5 min. and then subsequently subjected to exposure of a Nd:YVO_4 laser in a Q-switched mode. A 44 mJ/cm^2 of the dose was exposed onto the sample (45 sec. of exposure time per single exposure) before post exposure bake (PEB) was applied at 75 ^oC for 4 min.

Table S1 The analysis of polymerization results for the synthesized polymers via GPC and H-NMR data.

	Feed ratio (POSS mol%)	Product ratio (POSS mol%)	Initiator (mol%)	M_w	DP
PGMA -1	0	0	0.05	143k	1006
PGMA -2	0	0	0.1	101k	710
PGP-1	4.76	1.56	0.1	110k	712
PGP-2	9.09	3.03	0.1	157k	950
PGP-3	16.67	5.56	0.1	136k	732
PAP	100	100	0.1	4,791	5

The product mole ratio of each component was calculated using the intensity of the peaks at 0.6 ppm and 3.2 ppm for A1-POSS and GMA, respectively, in the H-NMR data. All practical ratios are about one-third of the feed ratio. This can be attributed to the steric hindrance of huge A1-POSS monomers that interrupts the participation of A1-POSS in copolymerization. All words, "PGMA", in the text of this report indicate PGMA-1 in **Table S1**.

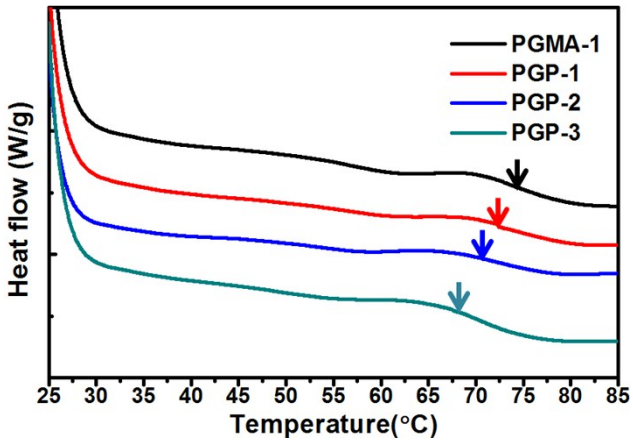

Fig. S1. T_g values of PGMA and synthesized PGPs confirmed via DSC.

T_g values of the synthesized polymers were decreased as the content of isobutyl POSS increases since POSS serves as an inert diluent of the dipole-dipole interaction of GMA molecules.

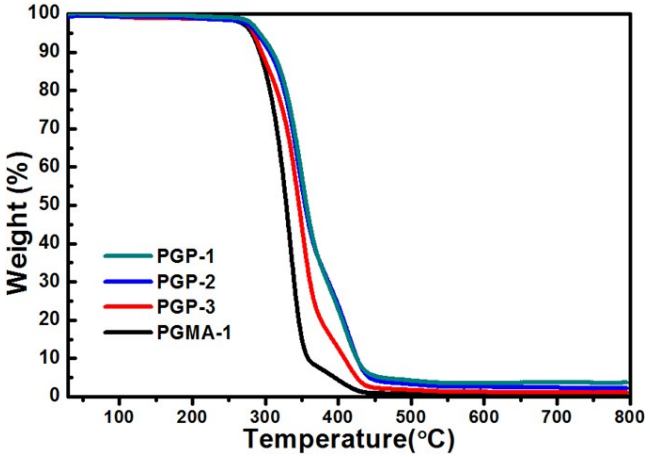

Fig. S2 Thermogravimetric analyses showing the thermal properties of synthesized PGPs.

Thermogravimetric analyses were conducted from 30 °C to 795 °C in a N_2 atmosphere. The pure PGMA has 5% weight loss (T_{dec}) at a temperature of 294 °C and has no remnant when the temperature reaches 800 °C. For PGPs, the T_{dec} and char yield increase with an increase of POSS content, indicating increased thermal stability of synthesized PGP copolymers.

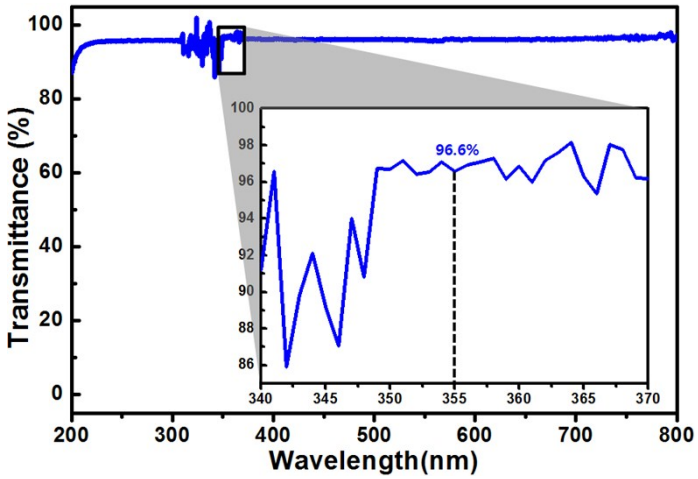

Fig. S3 The transmittance of the 100 µm-ultrathick PGP film confirmed via UV-Vis spectrophotometer.

The transmittance of the pure PGP film without photo-acid generator (PAG) was about 96.6% at the 355 nm which corresponds to wavelength of the irradiated laser light for photolithography.

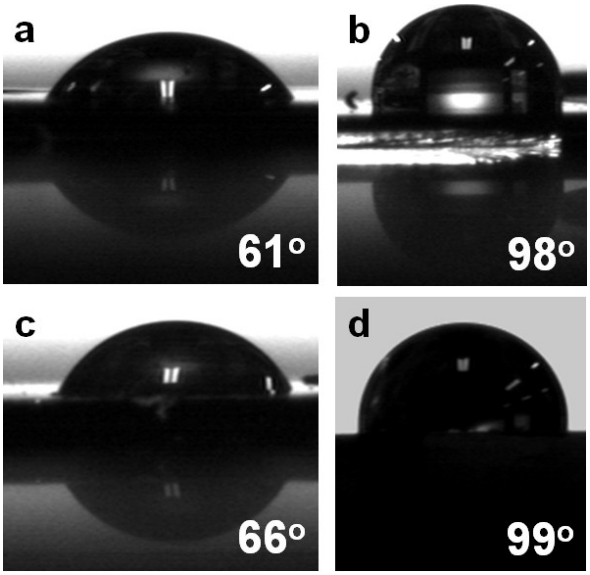

Fig. S4 Contact angle of PGMA (a: unpatterned structure, c: patterned structure) and PGP-2 (b: unpatterned structure, d: patterned structure) films.

Hydrophilicities of PGMA and PGP-2 films before and after patterning steps were confirmed by a contact angle investigation. PGP-2 has a much higher contact angle than PGMA films and the submicron patterned films have a higher contact angle than the bulk films.

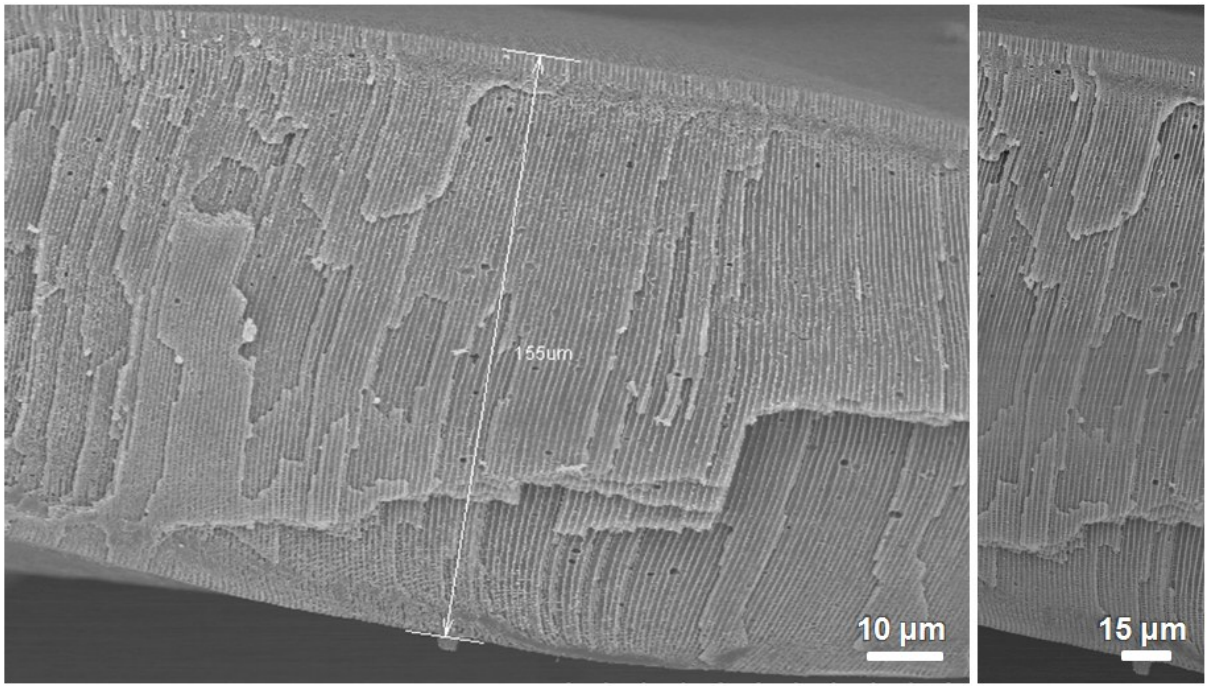

Fig. S5 SEM image of a square patterned submicron structure over 150 µm.

Submicron structure with an ultrahigh thickness over 150 µm was also made (slightly twisted and collapsed shape due to incomplete crosslinking density at the bottom of the film). The samples were broken with tweezers after freezing in liquid nitrogen to check the morphology of the entire thick-surface of the sample under a SEM.

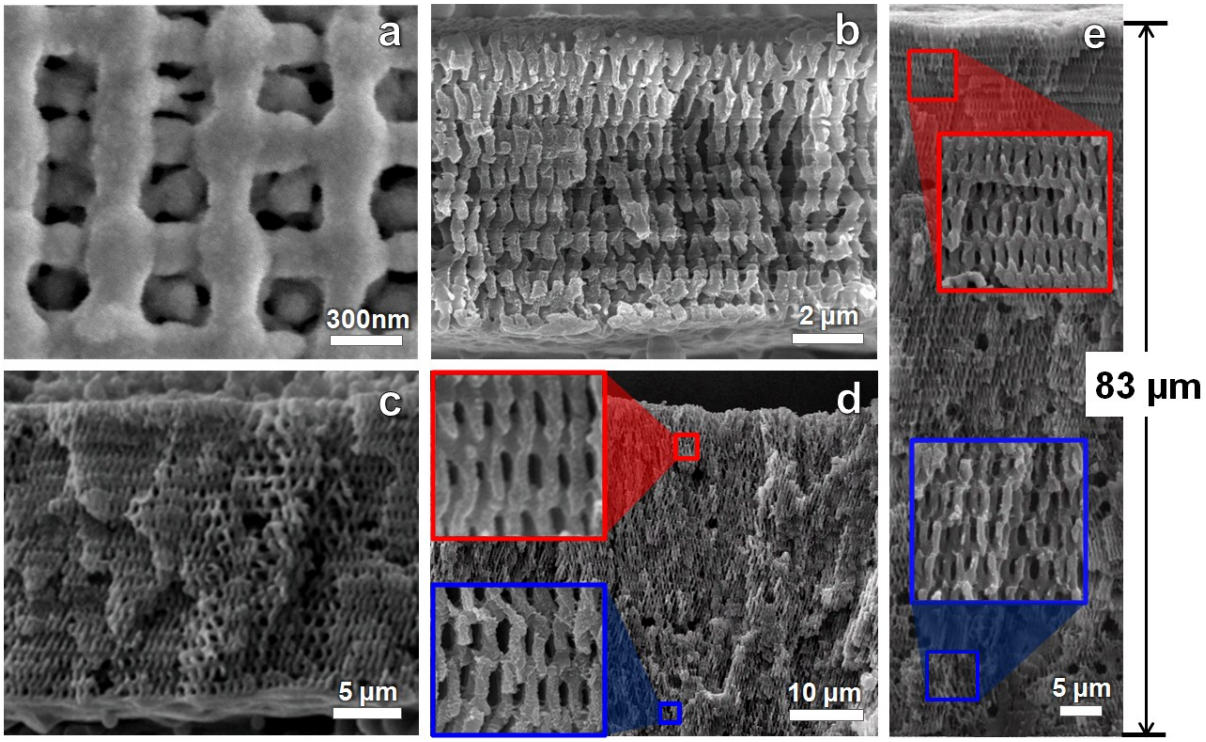

Fig. S6 SEM images of the holographic patterned submicron structures with various thicknesses. (a) Top view and cross-section view of (b) 8 µm, (c) 20 µm, (d) 50 µm and (e) 83 µm. The inset is the high magnification image.

Proximity-field nanopatterning method using a periodically patterned phase mask was employed to fabricate 3D-holographic patterned submicron structures. The top view image is shown in **Fig. S6a** and the thicknesses of submicron structures were 8, 20, 50, and 83 µm, as shown in **Fig. S6b-e**. These submicron structures indicate that the PGP photoresist could be applied to other various photolithography techniques as well.

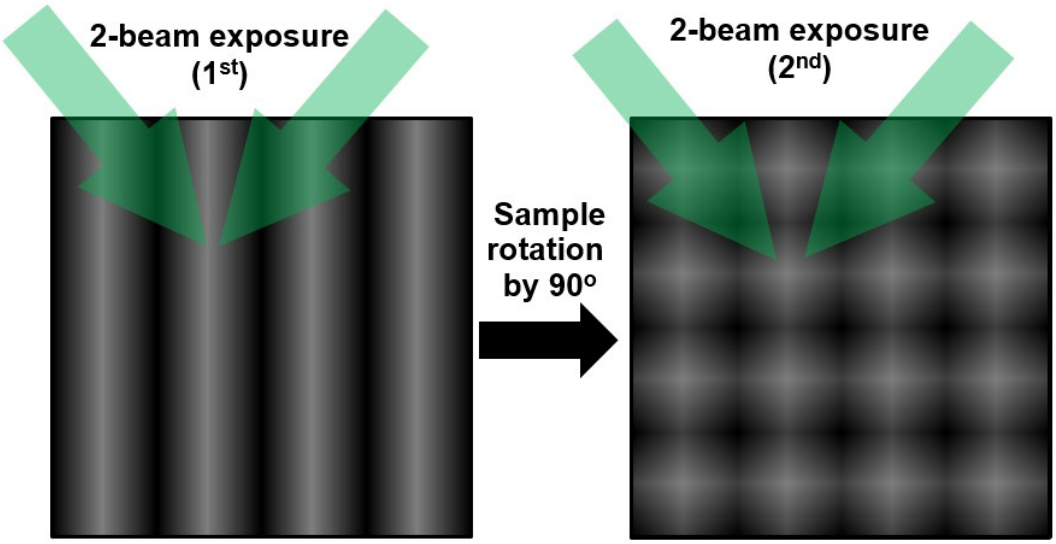

Fig. S7 Schematic of the fabrication of the square patterns via the double exposure of two laser beams with 90° rotation of the sample.

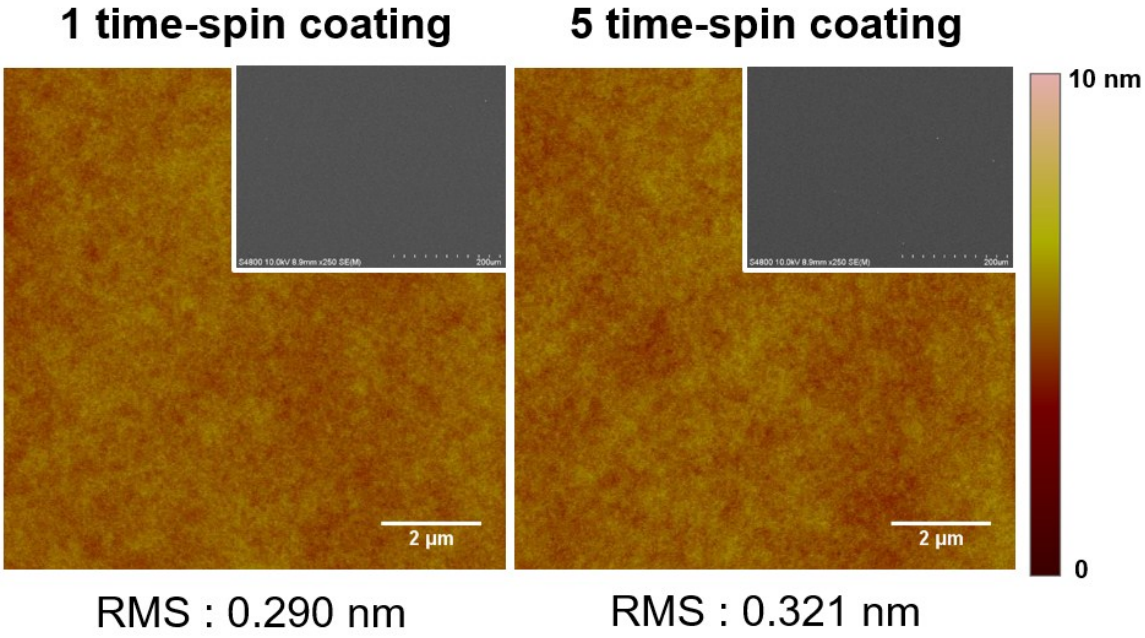

Fig. S8 AFM images of photoresist films with different thicknesses (10 x 10 μm area). The insets are large area SEM images.

Fig. S8 shows the root mean square (RMS) roughness values of the films made by repeated spin coatings of PGP-2. The root mean square (RMS) roughness values for the 1-time spin coated sample and the 5-time spin coated sample were 0.290 and 0.321 nm, respectively, implying that both samples possess quite uniform morphology considering the thickness of each sample is 12 μm and 107.5 μm, respectively.

Table S2 Thicknesses of the polymer films with respect to the concentration of the solution and the number of spin-coatings.

Material (Concentration)	The number of spin-coatings					
	1 time	2 times	3 times	4 times	5 times	6 times
PGMA (15%)	2.3 µm	3.7 µm	5 µm	7 µm	9.5 µm	12 µm
PGMA (30%)	12 µm	27 µm	45 µm	75 µm	97 µm	130 µm
PGP-1 (15%)	1.8 µm	3.2 µm	4.3 µm	5.7 µm	8.9 µm	10 µm
PGP-1 (30%)	8.3 µm	17 µm	28 µm	45 µm	62 µm	78 µm
PGP-2 (15%)	2.4 µm	4.2 µm	6.6 µm	9.5 µm	11.6 µm	17.2 µm
PGP-2 (30%)	12 µm	29 µm	54 µm	84 µm	107.5 µm	154 µm
PGP-3 (15%)	2.3 µm	3.7 µm	5.3 µm	8.6 µm	10 µm	14.3 µm
PGP-3 (30%)	10 µm	25 µm	36 µm	64 µm	85 µm	98 µm

Mechanical characterization of the submicron structure based on PGP-2 and PGMA films was confirmed using nanoindentation. A Berkovich tip and Oliver–Pharr method were used to investigate measurement and analyze the nanoindentation data to determine the respective elastic modulus and hardness.

The following series of equations were used to calculate the hardness values: $H_{OP} = \frac{P}{A}$ where P is the load and A is the calibrated projected contact area given by the area function, $A_c(h_c) = C_0 {h_c}^2 + C_1 h_c + C_2 {h_c}^{1/2} + C_3 {h_c}^{1/4} + C_4 {h_c}^{1/8}$ where the C_n are calibrated constants that account for imperfect Berkovich geometry. h_c is the contact depth given by the equation, $h_c = h - \varepsilon \frac{P}{S}$. Here, ε is a tip geometry specific constant set to 0.75 for the Berkovich tip and S is the measured contact stiffness during indentation.

Young's modulus was calculated using reduced modulus, E_r, is given by the equation, $E_r = \frac{\sqrt{\pi} \quad S}{2\beta\sqrt{A_c(h_c)}}$ where β is 1.034 for Berkovich tip and accounts for lack of axial symmetry. Young's modulus is then calculated by inserting corresponding Poisson ratio values and Young's modulus values to the equation, $\frac{1}{E_r} = \frac{1 - v^2}{E} + \frac{1 - v_i^2}{E_i}$.

References

1 D. Kim, H. C. Shim, T. G. Yun, S. Hyun and S. M. Han, Extreme Mechanics Letters, 2016, 9, Part 3, 439-448.